Journal of the European Ceramic Society 23 (2003) 387–398

www.elsevier.com/locate/jeurceramsoc

Acoustic emission characterisation of calcium aluminate cement hydration at an early stage

T.J. Chotard[a,b,*], A. Smith[a,*], D. Rotureau[a], D. Fargeot[a,b], C. Gault[a]

[a]*Groupe d'Etude des Matériaux Hétérogènes (GEMH, EA 3178), Ecole Nationale Supérieure de Céramique Industrielle, 47 à 73 Avenue Albert Thomas, 87065 Limoges Cedex, France*

[b]*Institut Universitaire de Technologie, Département Génie Mécanique et Productique, 2 allée André Maurois, 87065 Limoges Cedex, France*

Received 12 February 2002; accepted 12 April 2002

Abstract

In this paper, a new application of the acoustic emission (AE) technique is proposed. This non-destructive and in situ method, widely used in damage characterisation, permits us to follow the cement hydration at the early age from a few minutes to a few hours after mixing. The acoustic emission (AE) signals concerning a pure aluminous cement paste, (water to cement weight ratio = 0.4; temperature of measurement: 20 °C) were recorded and analysed. A specific treatment of data deduced from a fracture process identification procedure was applied. Different filters were set on the AE signal duration based on the characteristic of amplitude distribution. From the value of AE signal amplitude, correlation with physical and chemical changes were found.. Based on the experiments, the relationship between the AE characteristics recorded during the tests and the different mechanisms, which take place during setting, was emphasised. The results showed that the new application of the AE technique can be considered as a valuable tool to study the hydration of a cement at young age.

Keywords: Acoustic emission; Calcium aluminate cement; Cement; Hydration; Mechanical properties

1. Introduction

Calcium aluminate cements are widely used for many special applications in the construction and refractory industries due to their ability to gain strength rapidly and to withstand aggressive environments and high temperature.[1–3] The long-term behaviour of a cement paste is closely related to its state at an early age and in particular its hydration behaviour. The knowledge concerning this period is essential[4–6] in order to forecast the performance in service of these cement-based systems. Until today, different types of experimental techniques have been developed to characterise the hydration of these pastes. These techniques can be separated into two categories: ex situ techniques (X-rays diffraction, differential thermal analysis, thermogravimetric measurements), and in-situ methods such as proton and aluminium nuclear magnetic resonance,[7] neutron diffraction[8–10] or ultrasonic measurements.[11–13] Experimentally speaking, the development of new non-destructive and in situ techniques in order to follow the physical and chemical changes which occur during the hydration of a fresh cement paste is a real challenge. In this paper, we wish to present how the acoustic emission (AE) technique can provide useful information about cement hydration. AE has already proven its reliability for characterising the onset of free surfaces for phenomena like microcracking, crystallographic changes, opening of porosity or creation of new layers through corrosion, solidification processes in alloys; it concerns materials that are submitted to different types of solicitations such as mechanical loading, thermal cycles or corrosion.[14–20] The major advantages of AE technique are the following: (i) a continuous and in situ monitoring capability, (ii) the possibility to investigate, in one go, the whole volume of a structure with a limited number of sensors. Recently, AE has also been applied to study crack extension in concrete structures.[21,22]

Different attempts to detail the hydration mechanism in fresh Portland cement pastes during 1 or 2 h after

* Corresponding authors.
E-mail addresses: t.chotard@ensci.fr (T.J. Chotard), a.smith@ensci.fr (A. Smith).

0955-2219/02/$ - see front matter
PII: S0955-2219(02)00152-8

mixing have been reported in the literature.[23,24] They dealt with the component of ultrasonic signal that is transmitted inside the material, which can be, acoustically speaking, called an "active technique". The AE technique, reported in this work, is a "passive technique" which only considers the AE signals generated by the physical and chemical changes that occur in the cement paste during the first 24 h. In fact, the development of techniques for characterising, in real time, the stiffening of cement based materials is of industrial interest. It is important to remember that the present characterisations are done without applying any external load on the system under test.

2. Experimental procedure

2.1. Preparation of the cement paste

The cement is a commercial aluminous material (Secar 71) whose composition and physical characteristics are given in Table 1.

The particle size distribution ranges between 0.3 and 100 μm with an average size around 10 μm. The results presented in this paper refer to one cement manufactured at a given date and stored for a short period. A cement paste has been prepared with a water-to-cement weight ratio (W/C) equal to 0.4 and is noted SE040. This paste has been mixed according to the normalised procedure No. CEN 196–3. Prior to mixing, the constituents are kept at the mixing temperature for 12 h. After mixing, the paste was poured in a silicone foam mould (100×100×30 mm) prior to AE measurements. Dimensions of the mould have been chosen in order to be representative in volume. Silicone foam has been selected since it can follow the shrinkage of the cement paste during setting. A possible separation between the mould and the tested material is then reduced and the related parasite noise is avoided. The reproducibility of data has been checked with several pastes from the same cement. The characterisations have been carried out at 20 °C and 95% relative humidity.

Table 1
Chemical composition, either in nature of cementitious phase or in oxide, for the cement

Chemical composition			Percentage (wt.%)
Cementitious	phase	$CaAl_2O_4$ (or CA)	56
		$CaAl_4O_7$ (or CA_2)	38
		$Al_2O_3\alpha$	< 6
		$Ca_{12}Al_{14}O_{33}$ (or $C_{12}A_7$)	< 1
Oxide		CaO	26.6–29.2 wt.%
		Al_2O_3	69.8–72.2 wt.%

2.2. Acoustic emission

2.2.1. Background

Acoustic emission is a technique to monitor flaw formation and failures in structural materials. It has been used either at the laboratory level or industrial scale. Moreover, this method has been developed and applied in numerous structural components, such as steam pipes and pressure vessels, and in the research areas of rocks, composite materials, and metals. Acoustic emission (AE) is defined as "the class of phenomena whereby transient elastic waves are generated by the rapid release of energy from localised sources within a material (or structure) or the transient waves so generated". When a material is submitted to stresses (such as mechanical stresses, electric transients, etc.), acoustic emission can be generated by a variety of sources, including crack nucleation and propagation, multiple dislocation slip, twinning, grain boundary sliding, Barkhausen effect (realignment or growth of magnetic domains), phase transformations in alloys, debonding of fibres in composite materials or fracture of inclusions in alloys.[25–29]

In the case of concrete structures submitted to mechanical loading, AE events occur when cracks develop in the concrete and stress waves are emitted.[21,22] Research activities about AE have been applied to concrete either to characterise crack development or to monitor structure. Concerning the first aspect, AE has been used to observe the fracture process zone (FPZ) that develops ahead of the crack tip,[30] to describe the fracture mechanisms or to locate the cracks and their type of propagation.[31] Conventional AE source location methods are typically used to spatially locate crack development,[32] whereas moment tensor analysis has been applied to identify the location of the source and orientation of the damage.[33] With respect to the second aspect, several researchers have suggested the use of AE either to assess the degree of damage or as a method to monitor structural integrity.[34] In the present work, we propose a new use of AE. The technique will be devoted to record the elastic waves emitted during the physical and chemical changes that happen throughout the hydration of the cement paste. The specificity here is of two fold: (i) characterisation is done on a paste that transforms into a solid, (ii) no external load is applied on the system under study.

The potential of acoustic emission for providing reliable information and the ease with which it is applied for in situ testing depend largely on the available AE instrumentation. Significant improvements and modifications have been made on acoustic emission systems including features for numerical acquisition and analyses. From the emitted signals, different data can be extracted, namely number of counts, number of hits, rise time, peak amplitude, etc. Different types of analysis can

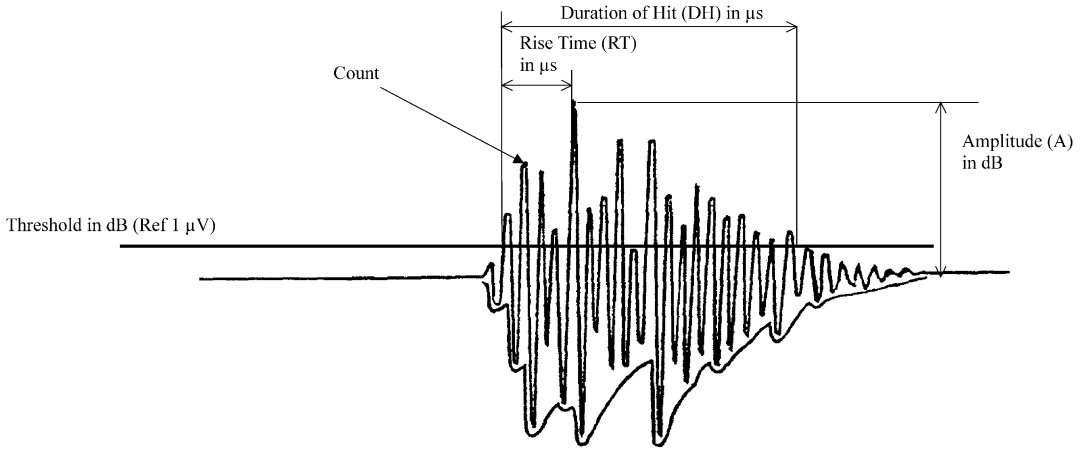

Fig. 1. Typical AE signal recorded with its associated characteristics.

also be done concerned with amplitude, duration, energy and frequency. When coupled with normalised mechanical testing of materials, AE enables the determination not only of the existence of damage, but also of the type and extent of damage. From this information, attempts have been made to infer the location of specimen failure and the probable mechanisms of failure.

2.2.2. Experimental set-up

The acoustic emission system used in this study is a AEDSP-32/16 MISTRAS digital system from Physical Acoustics Corporation. This system allows the waveform and the main feature parameters well known in AE study such as count, hit, rise time, duration of hit, count to peak, amplitude (in dB), to be recorded. Fig. 1 presents different AE features extracted from the signal waveform.

The plug-in filter of this system has a bandwidth from 100 to 1200 kHz. Two sensors (PAC MICROPHONE R15), one test sensor and one reference sensor, with a bandwidth from 50 to 250 kHz, are connected through preamplifiers (EPA 1220A). The reference sensor is used in order to record noises due to the electromagnetic environment and to eventually subtract these parasite signals from the one recorded on the test sensor. The preamplifiers provide 40/60 dB gain (switch select) and operate with either single ended or differential sensor. A coupling fluid (Dough 428 Rhodorsil Silicone) is used to have an airless and flawless contact between the transducer and the specimen. Fig. 2 shows the experimental set-up used in this study.

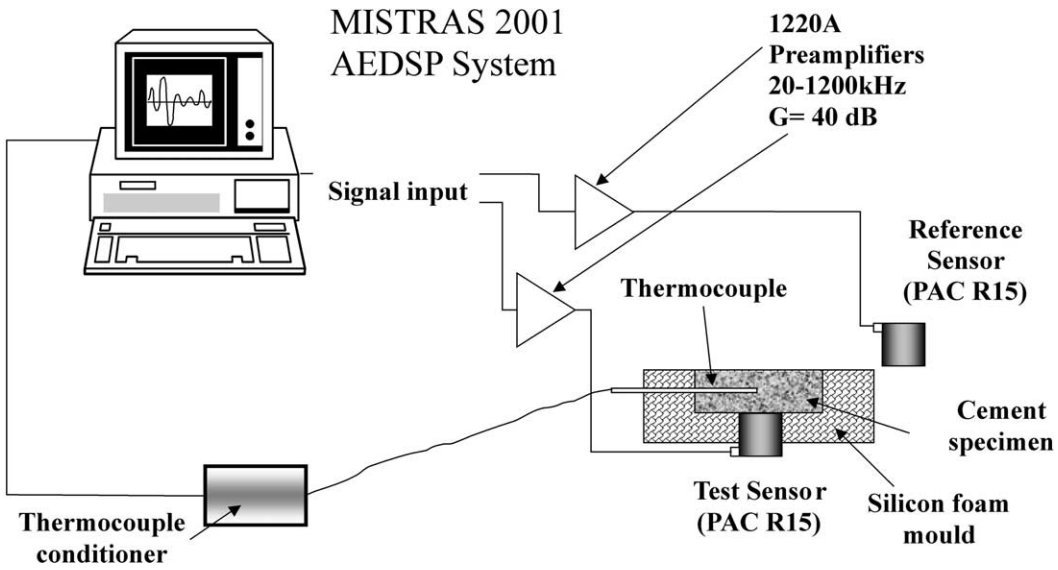

Fig. 2. Experimental set-up for AE measurements.

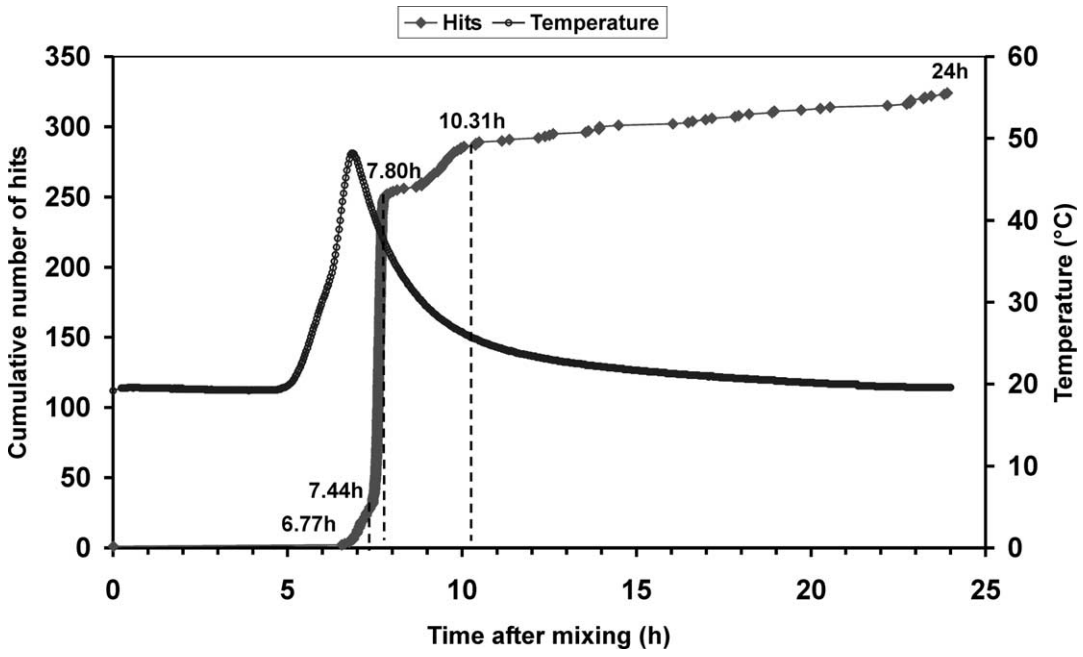

Fig. 3. AE cumulative number of hits and internal temperature as a function of time after mixing.

3. Results and discussion

3.1. Amplitude analysis

Fig. 3 presents a typical curve reporting the variations of both the AE cumulative hit and internal temperature for SE040 specimens as a function of time after mixing. In order to characterise the difference in AE activity occurring during the setting period, we calculated the hit rate which is defined as $\frac{\partial(AE \text{ cumulative number of hits})}{\partial t}$ and the values are reported in Table 2. From these data, five periods can be distinguished. During the first one (from 0 to 6.77 h) no acoustic emission activity is recorded. If we look at the temperature variations in the same interval, we notice that the temperature starts increasing 5 h after mixing water and cement. The first five hours correspond to the dormant period and it has been already characterised[35] by electrical measurements at high frequency (1 MHz–1.8 GHz). During this stage, a small number of hydrates starts to nucleate. It is important to note that this small amount of hydrates cannot be detected during this stage by conventional ex situ techniques such as X-ray diffraction (XRD), differential thermal analysis (DTA).[13] After 5 h, we observe a strong rise of the internal temperature reaching a maximum of 52 °C at approximately 6.90 h. It is well known that temperature is a good marker for the hydration reaction and that the exothermic peak is characteristic of the start of the massive hydration process. During the second period, from 6.77 to 7.44 h, the hit rate is about 52 hits/h. This parameter reaches its maximum (≈600 hits/h) during the third period (from 7.44 to 7.80 h). This stage is characterised by a large variation of the AE cumulative hit. Indeed more than 70% of the total AE hit number is recorded at 7.80 h. The last two periods, from 7.80 to 10.31 h and from 10.31 to 24 h, correspond to lower values of the hit rate compared to the previous ones since they are equal to 16 and 2 hits/h, respectively.

Table 2
Values of hit rate for the different time periods

Time period	Number of hits	Time delay	Hit rate (h^{-1})
0–6.77 h	0	6.77 h	0
6.77–7.44 h	35	0.67 h	52.2
7.44–7.80 h	215	0.36 h	597.2
7.80–10.31 h	40	2.51 h	15.9
10.31–24 h	30	13.69 h	2.2

The variations of the cumulative AE signal energy (in attojoules) as a function of time after mixing are plotted in Fig. 4. Two similarities with Fig. 3 can be pointed out: (i) division of the curve in the same five time domains, (ii) similar proportion of the total AE signal energy (around 70%) obtained at 7.80 h after mixing. These analogies can be easily emphasised by plotting the cumulative energy of AE signal versus the cumulative hit data (Fig. 5). Every point where there is a jump on the curve is related to a notable variation of these two parameters and it occurs at the end of each time period that we have previously defined. The number of cumulative counts vs. time curve (Fig. 6) also shows a shape which is similar to the cumulated hit vs. time curve. All these observations tend to demonstrate the existence of

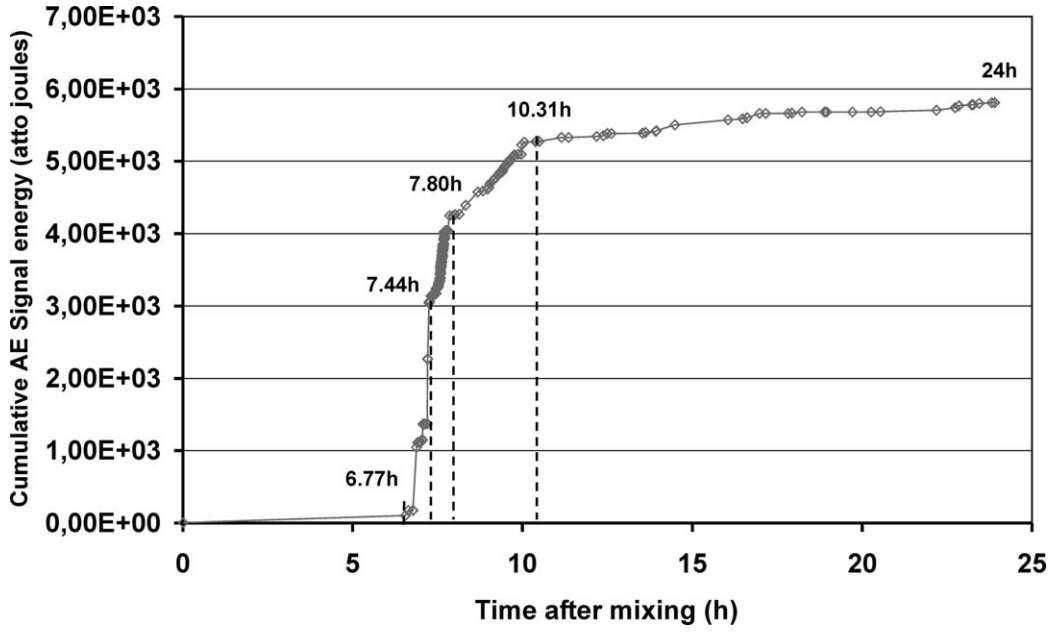

Fig. 4. AE cumulative signal energy as a function of time after mixing.

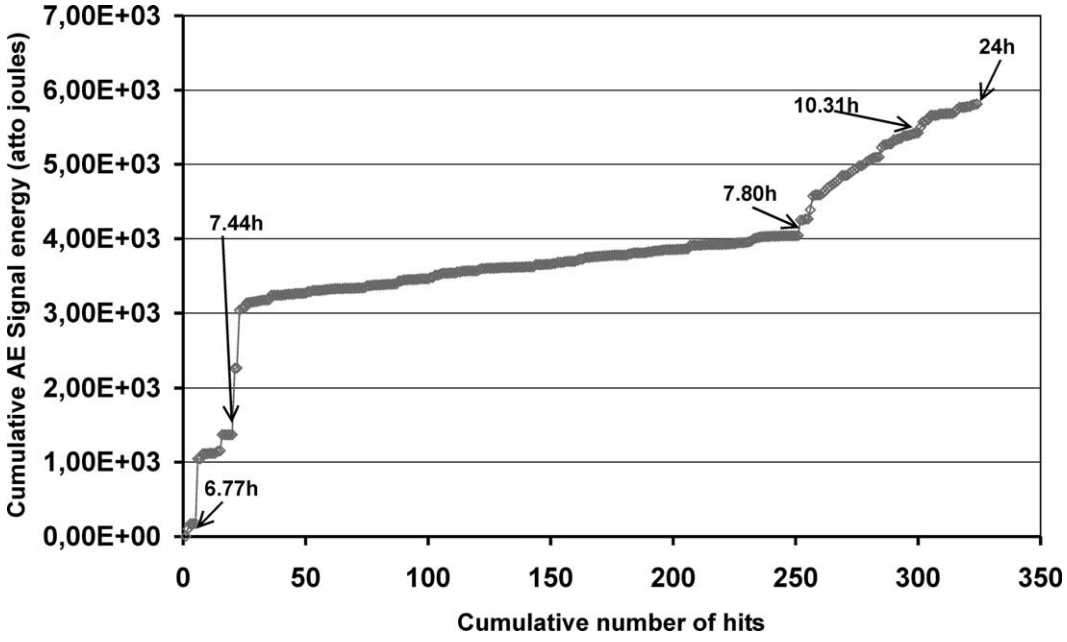

Fig. 5. AE cumulative signal energy as a function of cumulative hit.

a close correlation between the AE activity (hit and count), the type of AE activity (high or low AE signal energy) and the time of AE occurrence. For each time periods, we have applied the procedure described by Wu et al.[36] to analyse our data. This procedure is described below.

These authors have characterised by AE the fracture process of mortars, concrete and steel fibbers reinforced beams after introducing damage in their materials via a three-point bending test on single edge notched specimens. They have emphasised a relation between specific mechanism of fracture processes and the value of AE parameters extracted from the recorded signal. The hypothesis are the following:

(i) for the same AE activity, the higher the energy it emits, the higher the amplitude and the longer its duration are,
(ii) AE activities associated with the same mechanism have the same characteristics.

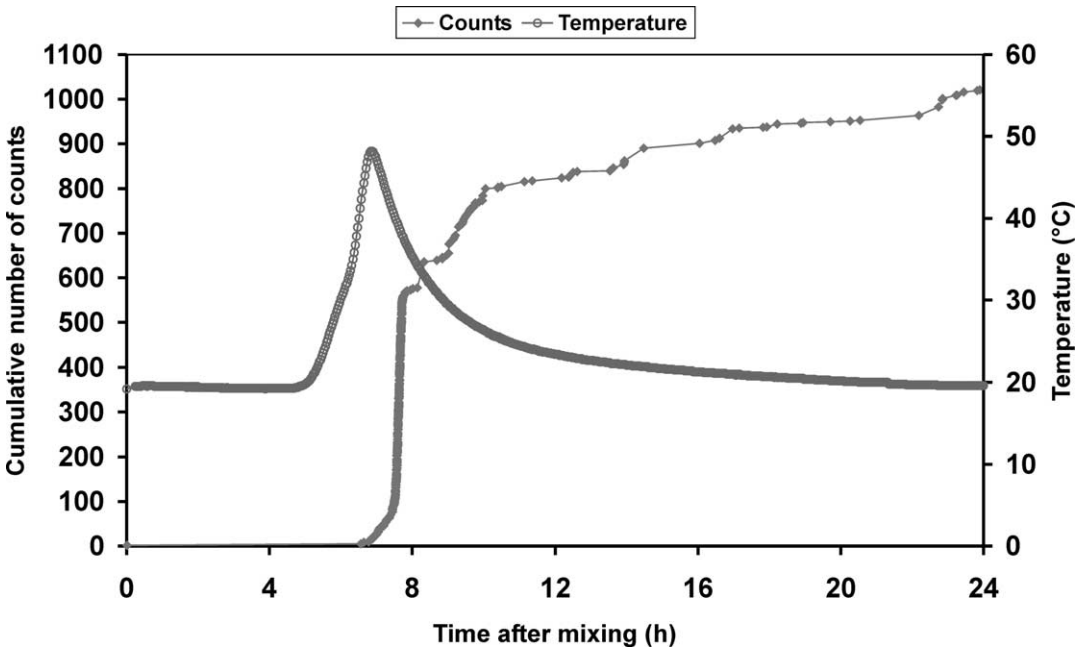

Fig. 6. AE cumulative number of counts and internal temperature as a function of time after mixing.

In order to isolate the different AE characteristics produced by the various fracture mechanisms, different time filters were set on the AE duration; these filters correspond to duration of the order of μs. When a given duration is selected, they adopt the following procedure (Fig. 7): the authors plot the number of counts and the number of hits vs. amplitude (in dB). If the amplitude values associated with the maximum of these two histograms, namely A and B are not similar, they define another time filter and repeat the plots. When $A = B$, they then plot the hits vs. counts histogram and look at the value of counts at the maximum of the histogram, C. The same procedure is repeated for the consecutive signal of AE activity that appear during the course of the experiment. The authors estimate an average value of count per hit, D, for each signal within the specified time filter. When $C = D$, they conclude they have identified one fracture mechanism where acoustic activity corresponds to the specific time filter. If $C \neq D$, no specific fracture mechanism can be proposed. With respect to our data, considering the hypothesis enounced by Wu et al., a time filter on the hit duration feature was applied and for each specific time domain. Table 3 summarises the result of this identification procedure. It is important to note that more than 70% of the total amount of hit (232) has been treated. Less than 30% (92) of the total amount was not computed due to the impossibility to classify them under a specific hit duration time filter. The first comment we can make is a good correlation between the maximum counts/hit value (C in Fig. 7) and the average value of counts per hit (D in Fig. 7). Although the number of treated hits is relatively low compared to the number treated in Wu's study, the reliability of the results is acceptable since the maximum dispersion is less than 10%. Secondly, two specific types of AE signal are present in each selected time period and up to 24 h. These signals have the following characteristics:

a. duration = 3–6 μs, peak amplitude = 38–39 dB, amplitude range from 35 to 40 dB, 2 counts/hit,
b. duration = 7–10 μs, peak amplitude = 40–41 dB, amplitude range from 36 to 42 dB, 4 counts/hit.

For these two types of signals, the hypothesis of a simple associated mechanism can be proposed. It is well known that in the cement paste, water fills up a capillary network. During hydration, this water can be consumed by the chemical reaction between water and cement (Fig. 3). The release of energy during the progressive emptying of this capillary network can induce a propagation of an elastic wave in the medium and consequently a noticeable AE activity. The contribution of these signals to the total number of hits is more important for the first two periods (up to 7.80 h) where the hydration reaction is significant and probably the consumption of water is maximum than afterwards. Indeed, after 7.80 h, when the material is rigid, hydration reaction progresses slowly.[13] Thirdly, we observe the occurrence of three other types of signal named (c), (d) and (e) with the following characteristics:

c. duration = 11–25 μs, peak amplitude = 43 dB, amplitude range from 38 to 45 dB, 5 counts/hit,

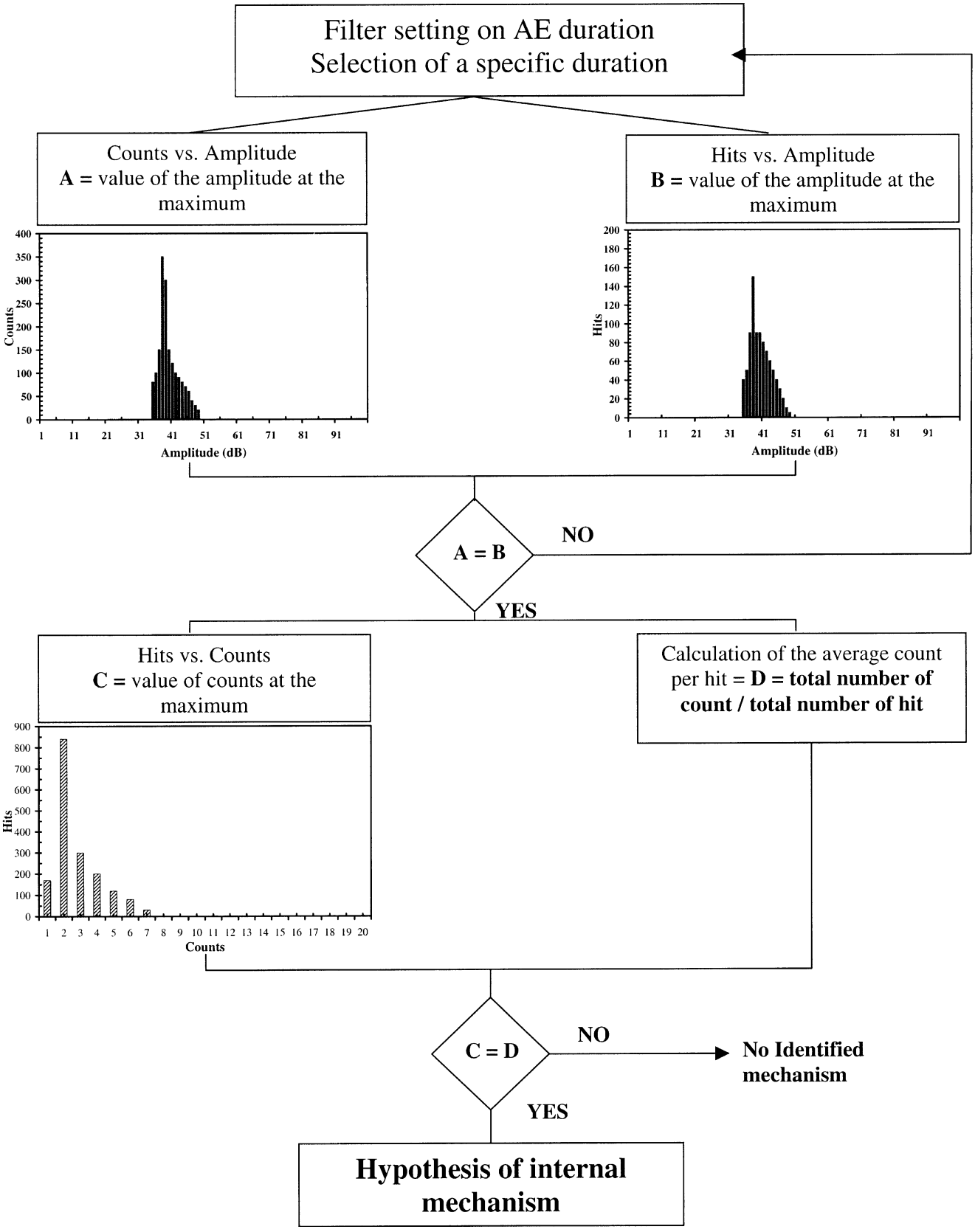

Fig. 7. Schedule of the mechanism identification procedure.

Table 3
AE parameter characteristics for each time period. The data concern 72% of the total amount of hits

Time period	Amplitude distribution (Histogram data)							
	Hit duration (μs)	Peak (dB)	Range (dB)	Max of counts/hits	Average count/hits	Hits	% Of total hits	Counts
0–6.77 h	(a) 3–6	38	35–39	2	1.8	10	3.1	18
	(b) 7–10	39	36–40	4	3.4	5	1.5	17
6.77–7.44 h	(a) 3–6	39	36–39	2	1.8	19	5.9	35
	(b) 7–10	40	37–40	4	3.8	10	3.1	38
	(c) 11–25	43	38–45	5	5.3	3	0.9	16
7.44–.80 h	(a) 3–6	39	36–40	2	2.1	21	6.5	44
	(b) 7–10	41	37–42	4	3.9	35	10.8	135
	(c) 11–25	44	39–47	5	4.9	60	18.5	293
	(d) 26–58	47	40–48	7	6.8	10	3.1	68
	(e) 59–200	56	47–56	10	9.8	5	1.5	49
7.80–10.31 h	(a) 3–6	38	36–39	2	1.9	8	2.5	15
	(b) 7–10	39	37–41	4	3.60	13	4.0	47
	(c) 11–25	41	38–46	5	4.9	10	3.1	49
10.31–24 h	(a) 3–6	38	35–39	2	2.2	6	1.8	13
	(b) 7–10	40	36–41	4	3.9	8	2.5	31
	(c) 11–25	44	39–45	5	5.1	9	2.8	46

d. duration = 26–58 μs, peak amplitude = 47 dB, amplitude range from 40 to 48 dB, 7 counts/hit,
e. duration = 58–200 μs, peak amplitude = 56 dB, amplitude range from 47 to 56 dB, 10 counts/hit.

The result of this procedure shows that three distinctive types of signal can be identified. The possible mechanisms associated to these signals are the precipitation of small germs of hydrates, the growth of crystalline phases and the onset of microcracking. Investigations are currently in progress to have a non equivocal relation between the AE signal and the type of mechanism. Several attempts have already been done in order to characterise the acoustic emission activity associated with physical and chemical engineering processes.[37] We can also point out that type (d) and (e) signals only occur during the period when the paste strongly hardens (7.44–7.80 h). The last comment concerns the plot of AE cumulative signal energy versus the cumulative number of hits (Fig. 5). We can note that the different time periods previously determined in Figs. 3 and 4 are also well quoted. The time period between 7.44 and 7.80 h is characterised by a high number of hit and a low AE cumulative signal energy. This kind of curve is very helpful in order to determine the different "stages" in AE which can occur during the material process.

3.2. Frequency analysis

Let us examine now the wave propagation problematic during the setting of a paste. Just after mixing, the cement paste is a concentrated aqueous suspension of clinkers and can be considered as a "water like medium". During this stage, the longitudinal (compression mode) wave propagates with a velocity and an attenuation value given by Johnson et al.[38] The transverse (shear mode) wave cannot propagate in such a medium. From the percolation threshold, the rigidity of the paste is sufficient to allow the transverse wave to propagate and consequently the amplitude of this wave grows notably. At a very young age, the dissipative character of the cement paste can be modelled by a linear viscoelastic behaviour. In this case, the elastic moduli are complex and frequency dependant. For example, the complex shear modulus is a function of the wave pulsation and consequently the wave frequency as shown:

$$\bar{G}(\omega) = G'(\omega) + jG''(\omega) \tag{1}$$

where $G'(\omega)$is the storage modulus related to the potential elastic energy stored in the material and $G''(\omega)$ is the dissipation (loss) modulus related to the dissipated energy in the material. The causes of this dissipation are complex and numerous; we can quote the viscosity of the fluid or the diffraction of the acoustic waves by heterogeneous particles.

In an homogeneous and viscoelastic medium submitted to a sinusoidal excitation, we can distinguish different cases of dynamic response:

(i) For a perfect elastic solid, we have:

$$\bar{G}(\omega) = \frac{\bar{\tau}(t)}{\bar{\varepsilon}(t)} = G \tag{2}$$

where $\bar{\tau}(t)$ and $\bar{\varepsilon}(t)$ are the complex stress and strain, respectively, and G the elastic shear modulus in Pa. Considering Eq. (2) and (1), it appears that:

$$G'(\omega) = G \quad \text{and} \quad G''(\omega) = 0 \tag{3}$$

(ii) In the case of a Newtonian viscous liquid, we obtain:

$$\bar{G}(\omega) = \frac{\bar{\tau}(t)}{\bar{\varepsilon}(t)} = \eta \frac{\dot{\bar{\varepsilon}}(t)}{\bar{\varepsilon}(t)} = i\eta\omega \tag{4}$$

where η is the absolute viscosity in Pa.s. Considering here Eq. (4) and (1), we can deduce that:

$$G'(\omega) = 0 \quad \text{and} \quad G''(\omega) = \eta\omega \tag{5}$$

(iii) The third case presented here is related to the model of a Maxwell liquid. This model (and the model of Kevin–Voigt) takes into account the viscoelastic behaviour and can be representative of the rheological evolution of the cement when it transforms from a paste to a solid. At its viscous state the cement paste cannot be considered as a Newtonian viscous liquid due to its thixotropic character. For this configuration, we have for the total stress τ and strain ε:

$$\frac{\mathrm{d}\varepsilon}{\mathrm{d}t} = J\frac{\mathrm{d}\tau}{\mathrm{d}t} + \frac{1}{\eta}\tau \tag{6}$$

where $J = 1/G$ is called the elastic compliance. Eq. (6) is called the rheological equation of a Maxwell liquid. Using the initial conditions such as for $t<0$: $\tau = 0$ and $\varepsilon = 0$, we obtain the resolution of Eq. (6) as:

$$\varepsilon(t) = J\tau(t) + \frac{1}{\eta}\int_0^t \tau(t)\mathrm{d}t \tag{7}$$

Let us consider that the stress and the strain are defined as follows:

$$\tau(t) = \tau_0 e^{i(\omega t+\delta)} \quad \text{and} \quad \varepsilon(t) = \varepsilon_0 e^{i\omega t} \tag{8}$$

where τ_0, ε_0 are the maximum amplitude of the stress and strain respectively, $\omega = 2\pi f$, the pulsation, f the frequency of the wave, and δ, the phase difference between stress and strain. By combining Eqs. (7) and (8), the complex modulus is equal to:

$$\bar{G}(\omega) = \frac{\bar{\tau}(t)}{\bar{\varepsilon}(t)} = \frac{i\omega}{\frac{1}{\eta} + i\frac{\omega}{G}} = \frac{i\eta\omega}{1 + i\omega\frac{\eta}{G}} \tag{9}$$

or, if we note $\theta = \frac{\eta}{G}$ as the relaxation time of the Maxwell liquid:

$$\bar{G}(\omega) = \frac{\omega^2\eta\theta + i\omega\eta}{1 + \omega^2\theta^2} \tag{10}$$

By combining the terms in Eqs. (1) and (10), the values of the real and imaginary parts of the complex modulus $\bar{G}(\omega)$ are the following:

$$G'(\omega) = G\frac{\omega^2\theta^2}{1 + \omega^2\theta^2} \quad \text{and} \quad G''(\omega) = G\frac{\omega\theta}{1 + \omega^2\theta^2} \tag{11}$$

This can be simply re-written as:

$$\frac{G'(\omega)}{G''(\omega)} = \omega\theta = \omega\frac{\eta}{G} \tag{12}$$

For a cement, G is of the order of $5–7\times10^9$ Pa,[12] and the viscosity η is of the order of 10^{-1}–10^2 Pa.s when it is a paste and 10^{16}–10^{18} Pa.s when it is in its solid state.[39] Theoretically speaking, during the first few hours after mixing, the cement paste is in its viscoelastic state. During this stage if we consider Eq. (12) and assume that $\eta \approx 10^{-1}$ Pa.s and G the corresponding values of and $G \approx 6.10^9$ Pa, we obtain:

$$\frac{G'(\omega)}{G''(\omega)} << 1 \tag{13}$$

The intrinsic attenuation coefficient $\alpha(\omega)$ for a monochromatic wave, is given by:

$$\alpha(\omega) = \omega\sqrt{\frac{\rho}{2}\left(\frac{1}{\sqrt{G'^2(\omega) + G''^2(\omega)}} - \frac{G'(\omega)}{G'^2(\omega) + G''^2(\omega)}\right)} \tag{14}$$

with ρ the density of the medium. Consequently, if we introduce the condition deduced from Eq. (13) in Eq. (14), the attenuation coefficient becomes:

$$\alpha(\omega) \cong \omega\sqrt{\frac{\rho}{2}\left(\frac{1}{G''(\omega)}\right)} \tag{15}$$

The resulting value of $\alpha(\omega)$ shows that the higher the frequency is, the higher the attenuation coefficient is. In other words, the viscoelastic state acts as a low-pass filter for the ultrasonic waves which propagate inside the cement paste.

As the hydration progresses, the paste starts to stiffen and it changes from a viscoelastic to an elastic medium.

In this state, with respect to the associated values of η and G (10^{16} Pa.s and 6.10^9 Pa, respectively), we have:

$$\frac{G'(\omega)}{G''(\omega)} >> 1 \tag{16}$$

The new expression of the attenuation coefficient deduced from Eq. (14) is then:

$$\alpha(\omega) \cong \omega\sqrt{\frac{\rho}{2}\left(\frac{1}{G'(\omega)} - \frac{1}{G'(\omega)}\right)} \tag{17}$$

which indicates that this coefficient tends towards 0 when the material is in its elastic state. It is important to note that this coefficient will still remain low whatever the considered frequency of the propagating waves will be. Consequently, a significant contribution of the signal in the high frequencies can be observed. A small restriction must be done in the case of our study. Here, we only record the result of the propagation of an ultrasonic elastic wave throughout a medium. We do not control the type and the frequency of the emitted wave (longitudinal or transverse). The recorded signal are probably both a combination and a superposition of waves, initiated by internal phenomena already quoted, propagating through a heterogeneous medium where regions in a viscoelastic or an elastic state can be next to each other.

By carrying out a frequency treatment of our data, it is possible to characterise this change in the mechanical behaviour of the cement paste during setting. This frequency treatment is done by recording the entire waveform signal. A fast Fourier transform (FFT) has been applied to the waveform in order to represent the frequency spectrum (spectrum amplitude vs. frequency). For this study, three typical hits recorded at specific times (Hit No. 1: 7.04 h; Hit No. 2: 7.65 h; Hit No. 3: 11.14 h) were treated. Fig. 8 presents the frequency spectrum (FFT transform) of these hits. We observe a notable frequency shift from low frequencies (Fig. 8a) towards high frequencies (Fig. 8c) while the paste stiffens. Such an observation seems to be in accordance with the above discussion: the frequency shift corresponds to the low-pass filter character of the paste at the very young age. As the cement transforms from a viscoelastic to an elastic state, the frequency shifts towards higher values. This analysis takes into account the percentage of the total spectral energy by frequency range (here 100 kHz). Table 4 summarises this spectral analysis. The maximum of the percentage of total spectral energy is localised in the 0–100 kHz frequency range for hit No. 1 and moves towards 200–400 kHz for hit No. 3.

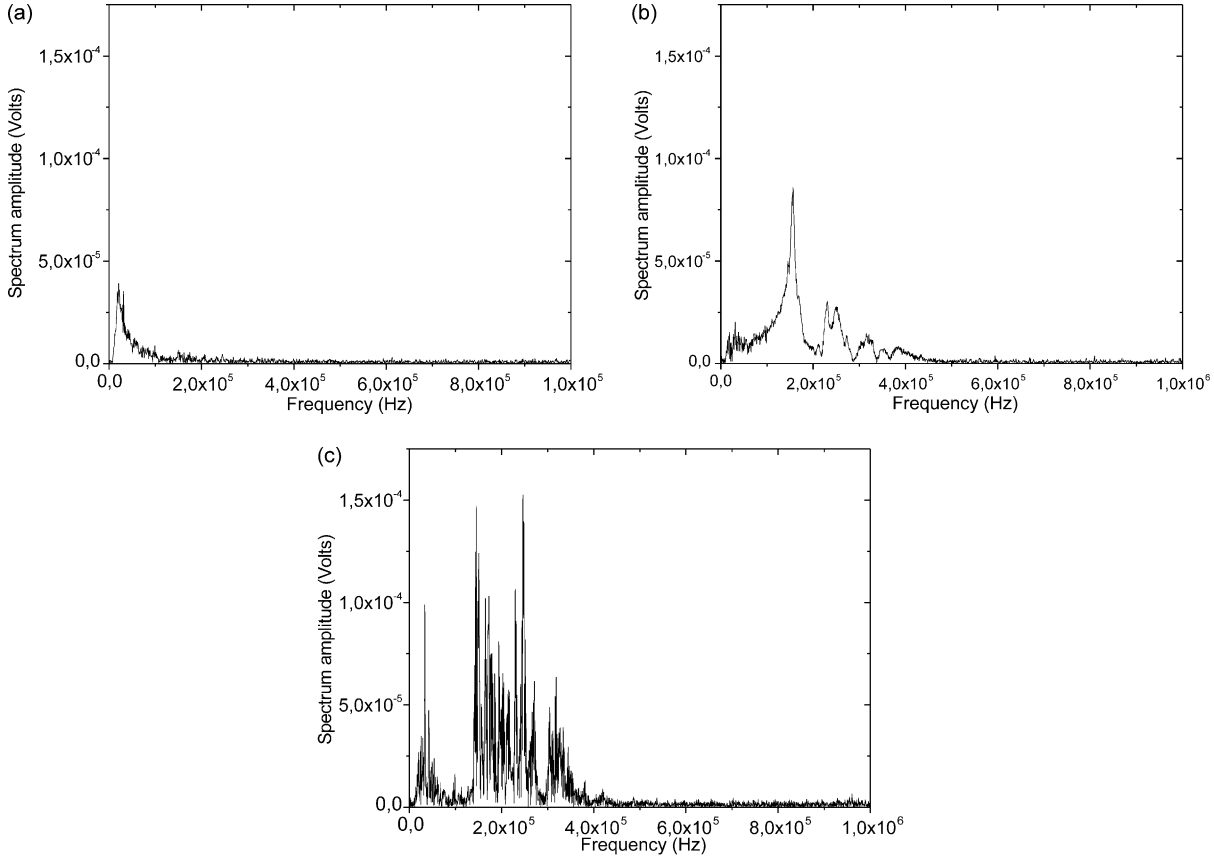

Fig. 8. Frequency spectrum (FFT transform) for AE hit recorded at: (a) 7.04 h; (b) 7.65 h, (c) 11.14 h.

Table 4
Frequency analysis for specific recorded hits

Frequency range	Percentage of total energy spectrum		
	Hit No. 1 (7.04 h)	Hit No. 2 (7.65 h)	Hit No. 3 (11.14 h)
0–100 kHz	51.7	15.0	10.8
100–200 kHz	10.9	43.8	33.0
200–300 kHz	7.1	19.7	30.8
300–400 kHz	5.6	10.7	14.4
400–500 kHz	4.6	3.4	2.6
500–600 kHz	3.9	1.7	1.7
600–700 kHz	4.1	1.4	1.5
700–800 kHz	3.9	1.3	1.6
800–900 kHz	4.0	1.5	1.6
900–1000 kHz	4.2	1.5	1.9

4. Conclusion

The results presented in this paper show that AE technique can be considered as a potentially interesting tool to characterise the early hydration of a cement paste (0–24 h). This "passive technique" allows a continuous and an in-situ monitoring of cement paste setting. Several points can be highlighted:

1. The characterisation of an AE activity closely related to the internal changes in the cement paste has been performed.
2. Experimental results indicate the existence of five different time periods in the AE activity.
3. Based on the experiments, a specific procedure has been adapted with a good reliability in order to distinguish the different AE signals taking place during each time period. The proposed mechanisms that are associated to these signals are the emptying of the capillary pores, formation of germs of hydrates, the growth of the hydrated phases and the development of microcracking closely related to the shrinkage of the paste.
4. The frequency analysis shows the change in mechanical behaviour of the cement paste from a viscoelastic to an elastic state. The frequency shift from 0–100 kHz to 300–400 kHz is related to the stiffening of the paste.

Further investigations will be made in order to characterise separately the internal mechanisms (hydration, conversion of hydrates, porosity onset, microcracking) on model materials by both amplitude and frequency analysis.

References

1. Scrivener, K. L., Cabiron, J. L. and Letourneux, R., High-performance concretes from calcium aluminate cements. *Cem. Conc. Res.*, 1999, **29**, 1215–1223.
2. Scrivener, K. L., Historical and present day applications of calcium aluminate cements. In *Calcium Aluminate Cements 2001*, ed. R. J. Mangabhai and F. P. Glasser. 2001, pp. 3–23.
3. Gessner, W., Recent researches on calcium aluminate hydration. In *Calcium Aluminate Cements 2001*, ed. R. J. Mangabhai and F. P. Glasser. 2001, pp. 151–154.
4. Capmas, A., Ménétrier-Sorrentino, D. and Damidot, D., Effect of temperature on setting time of calcium aluminate cements. In *Calcium Aluminate Cements*, ed. R. J. Mangabhai E. and F Spon. 1990.
5. Fujii, K., Kondo, W. and Ueno, H., Kinetics of hydration of monocalcium aluminate. *J Am. Ceram. Soc.*, 1986, **69**(4), 361–364.
6. Edmonds, R. N. and Majumdar, A. J., The hydration of monocalcium aluminate at different temperatures. *Cem. Conc. Res.*, 1988, **18**(2), 311–320.
7. Cong, X. and Kirkpatrick, R. J., Hydration of calcium aluminate cements: a solid-state ^{27}Al NMR study. *J. Am. Ceram. Soc.*, 1993, **76**(2), 409–416.
8. Barnes, P., Clark, S. M., Hausermann, D., Henderson, E., Fentiman, C. H., Muhamad, M. N. and Rashid, S., Time-resolved studies of the early hydration of cements using synchrotron energy-dispersive diffraction. *Phase Transitions*, 1992, **39**, 117–128.
9. Rashid, S., Barnes, P., Bensted, J. and Turrilas, X., Conversion of calcium aluminate cement hydrates re-examined with synchrotron energy-dispersive diffraction. *J. Mater. Sci. Lett.*, 1994, **13**, 1232–1234.
10. Rashid, S. and Turrillas, X., Hydration kinetics of $CaAl_2O_4$ using synchrotron energy-dispersive diffraction. *Thermochimica Acta*, 1997, **302**, 25–34.
11. Mayfield, B. and Bettison, M., Ultrasonic pulse testing of high alumina cement concrete. *Concrete, 1974, 36–38.*
12. Boumiz, A., Vernet, C. and Cohen-Tenoudji, F., Mechanical properties of cement and mortars at early ages. *Adv. Cem. Bas. Mater.*, 1996, **1**, 94–106.
13. Chotard, T., Gimet-Bréart, N., Smith, A., Fargeot, D., Bonnet, J.P. and Gault, C, Application of ultrasonic testing to describe the hydration of calcium aluminate cement at the early age. *Cem. Conc. Res.*, 2001, **31**, 405–412.
14. Barré, S. and Benzeggagh, M. L., On the use of acoustic emission to investigate damage mechanisms in glass-fibre-reinforced polypropylene. *Comp. Sci. Technol.*, 1994, **52**, 369–376.
15. Hamstad, M. A., Thompson, P. M. and Young, R. D., Flaw growth in alumina studied by acoustic emission. *J. Acous. Emis.*, 1987, **6**, 93–97.
16. Bakuckas, J. G., Prosser, W. H. and Johnson, W. S., Monitoring damage growth in titanium matrix composites using acoustic emission. *J. Comp. Mater.*, 1994, **28**, 305–328.
17. Berkovits, A. and Fang, D., Study of fatigue crack characteristics by acoustic emission. *Eng. Fract. Mech.*, 1995, **51**, 401–416.
18. Havlicek, F. and Crha, J., Acoustic emission monitoring during solidification processes. *J. Acous. Emi.*, 1999, **17**, 3–4.
19. Coddet, C., de Barros, G. and Beranger, G., Influence of thermal cycling between 20 and 400 °C on the oxidation of copper. In *Proceedings of the European Symposium.* 1981, pp. 417–426.
20. Coddet, C., Chretien, J. F. and Beranger, G., Investigation on the fracture mechanism of oxide layers growing on titanium by acoustic emission. *Titanium and Titanium Alloys: Scientific and Technological Aspects*, 1982, **2**, 1097–1105.
21. Ohtsu, M., Tomoda, Y. and Fujioka, T., Estimation of initial damage in concrete by acoustic emission. In *Fourth Far East Conference on NDT.* 1997.
22. Chen, H. L., Cheng, C. T. and Chen, S. E., Determination of fracture parameters of mortar and concrete beams by using acoustic emission. *Mater. Eval.*, 1992, **July**, 888–894.
23. Sayers, C. M. and Dahlin, A., Propagation of ultrasound through hydrating cement pastes at early times. *Adv. Cem. Bas. Mater.*, 1993, **1**, 12–21.

24. Sayers, C. M. and Grenfell, R. L., Ultrasonic propagation through hydrating cements. *Ultrasonics*, 1993, **31**(3), 147–153.
25. Prosser, W. H., Jackson, K. E., Kellas, S., Smith, B. T., McKeon, J. and Friedman, A., Advanced waveform-based acoustic emission detection of matrix cracking in composites. *Mater. Eval., 1995, 1052–1058*.
26. Suzuki, H., Takemoto, M. and Ono, K., The fracture dynamics in a dissipative glass fibber/epoxy model composite with AE source simulation analysis. *J. Acous. Emis.*, 1996, **14**, 35–50.
27. Pauchard, V., Brochado, S., Chateauminois, A., Campion, H. and Grosjean, F., Measurement of sub-critical crack-growth rates in glass fibbers by means of acoustic emission. *J. Mater. Sci. Lett.*, 2000, **19**, 2141–2143.
28. Ono, K. and Huang, Q., Pattern recognition analysis of acoustic emission signals. In *Progress in Acoustic Emission. VII*, The Jpn. Soc. For NDI. 1994, pp. 69–78.
29. Krietsch, T. and Bohse, J., Selection of acoustic emissions and classification of damage mechanisms in fiber composite materials. In *Progress in Acoustic emission XI*, The Jpn. Soc. For NDI. 1998, pp. 80–87.
30. Maji, A. and Shah, S. P., Process zone and acoustic emission measurement in concrete. *Exp. Mech.*, 1988, **March**, 27–33.
31. Li, Z. and Shah, S. P., Localisation of microcracking in concrete under uniaxial tension. *ACI Mater Journal*, 1994, **July–August**, 372–381.
32. Yuyama, S., Okamoto, T., Shigeishi, M. and Ohtsu, M., Quantitative evaluation and visualisation of cracking process in reinforced concrete by a moment tensor analysis of acoustic emission. *Mater. Eval.*, 1995, **June**, 751–756.
33. Ohtsu, M., Okamoto, T. and Yuyama, S., Moment tensor analysis of acoustic emission for cracking process concrete. *ACI Struct. Journal*, 1998, **March–April**, 87–95.
34. Uomoto, T., Application of acoustic emission to the field of concrete engineering. *J. Acous. Emis.*, 1987, **6**, 137–144.
35. Chotard, T., Gimet-Bréart, N., El Hafiane, Y., Smith, A. Bonnet JP, Abelard, P., Tanouti, B. and Blanchart, P. Electrical characterisation at high frequency (1 MHz–1 GHz) of an aluminous cement. *An. Sci. Mater*. 1991, **25**, *Suppl. 1* 297–302.
36. Wu, K., Chen, B. and Yao, W., Study on the AE characteristics of fracture process of mortar, concrete and steel-fibre-reinforced concrete beams. *Cem. Conc. Res.*, 2000, **30**, 1495–1500.
37. Boyd, J. W. R. and Varley, J., The uses of passive measurement of acoustic emissions from chemical engineering processes. *Chem. Eng. Sci.*, 2001, **56**, 1749–1767.
38. Johnson, D. L. and Plona, T. J., Acoustic slow waves and consolidation transition. *J. Acous. Soc. Am.*, 1982, **72**, 556–565.
39. Chappuis, J., Rheological measurements with cement pastes in viscometers: a comprehensive approach. In *Rheology of Fresh Cement and Concrete*, ed. P. F. G. Banfill. The British Society of Rheology, E and F Spon, London, 1990, pp. 3–12.